Enhanced energy transfer and multimodal vibration mitigation in an electromechanical acoustic black hole beam

Linli Zhang [1], Xiang Sun [1], Jennifer Dietrich [2], Gaetan Kerschen [2] and Li Cheng [1,]*

[1] *Department of Mechanical Engineering, The Hong Kong Polytechnic University, Hung Hom, Kowloon, Hong Kong SAR, P. R. China*

[2] *Department of Aerospace and Mechanical Engineering, University of Liège, Allée de la Découverte 9, B-4000 Liège, Belgium*

**Corresponding author: li.cheng@polyu.edu.hk*

Abstract: Owing to their unique energy focusing capability and high-frequency damping effects, Acoustic Black Hole (ABH) structures show promise for numerous engineering applications. However, conventional ABH structures are mostly effective only above the so-called cut-on frequency, a bottlenecking deficiency that needs to be addressed if low-frequency problems are of concern. Meanwhile, achieving simultaneous high frequency ABH effects and low-frequency vibration reduction is also a challenge. In this paper, electrical linear and nonlinear shunts are intentionally added to an ABH beam via PZT patches to tactically influence its dynamics through electromechanical coupling. Both numerical and experimental results confirm that the effective frequency range of the ABH can be broadened as a result of the electrical nonlinearity induced energy transfer (ET) from low to high frequencies inside the beam. However, increased nonlinearity strength, albeit beneficial to energy transfer, jeopardizes the linear dynamic absorber (DA) effects acting on the lower-order resonances. Solutions are exploited to tackle this problem, exemplified by the use of negative capacitance in the nonlinear shunts with the embodiment of parallel linear electrical branches. On top of the nonlinear ET effects, simultaneous DA effect is also achieved for the low-frequency resonant vibration mitigation. Studies finally end up with a design methodology which embraces the principle of ET and DA to tactically cope with different frequency bands. The final outcome is the broadband multi-modal vibration reduction and the breaking down of the frequency barrier existing in conventional linear ABH structures.

Keywords: Acoustic black hole; Electromechanical coupling; Electrical nonlinear shunt; Energy transfer; Dynamic absorber; Multimodal vibration mitigation

1. Introduction

Acoustic Black Hole (ABH) effect has attracted sustained interests in the scientific community over the past decade [1], due to the unique features it offers for manipulating flexural waves in thin-walled structures whose thickness profile is tailored according to a reducing power-law relationship. The wave energy can be trapped around the ABH tip [2], and then effectively dissipated by using a small amount of damping materials [3]. ABH structures have been explored for different engineering applications such as vibration control, structural sound radiation reduction and energy harvesting, *etc* [1, 4].

However, most existing research on ABH focuses on linear structures [4]. Even though linear ABHs exhibit remarkable and persistent energy focusing and damping enhancement at high frequencies, their deficiency at low frequencies, typically below the cut-on frequency, is still a major bottle-necking problem which hinders their applications. Reducing the frequency limit in a linear ABH structure would require an increase in the ABH size, such as the use of extended platform on the ABH tip [5] and the design of spiral ABH [6], With

limited success, these measures also affect the acceptance of the large-sized or complex structural design in engineering practice.

Exploration of geometric or intentional nonlinearities would offer a promising solution to this problem [7]. Due to the lack of tuning flexibility of mechanical nonlinearities such as vibro-impact and contact nonlinearity, electrical nonlinearity was intentionally introduced in an ABH beam in our previous work [8] as a novel nonlinear energy transfer device. It was demonstrated that a properly designed nonlinear shunt enables obvious cross-frequency energy transfer; and the transferred energy at high frequencies can be effectively dissipated through the damping of the ABH. The tuning flexibility offered by the electrical design can cater for specific structural modes in specific frequency ranges. However, it was also observed that the level of the energy transfer was limited and the direct effects on low-frequency vibration was barely observable due to the nonlinearity-impaired dynamic absorber (DA) effects. Therefore, it was difficult to conciliate the ET and DA effects simultaneously using the original shunt design.

Therefore, realizing enhanced cross-frequency ET while maintaining the DA effect to achieve broadband multimodal vibration mitigation is set to be the focus of this study. Considering the above, this paper targets a three-fold objective: (a) enhancing electromechanical coupling and ET in an ABH beam while maintaining DA effect to achieve low-frequency vibration mitigation; (2) establishing the underlying rationale which guides the electrical shunt design deployed the combined ET and DA effect to tactically cope with specific mitigation philosophies adopted for different frequency ranges.(c) proposing an example for comprehensive design based on the design principle to finally achieve broadband multimodal vibration mitigation.

2. Theoretical Model

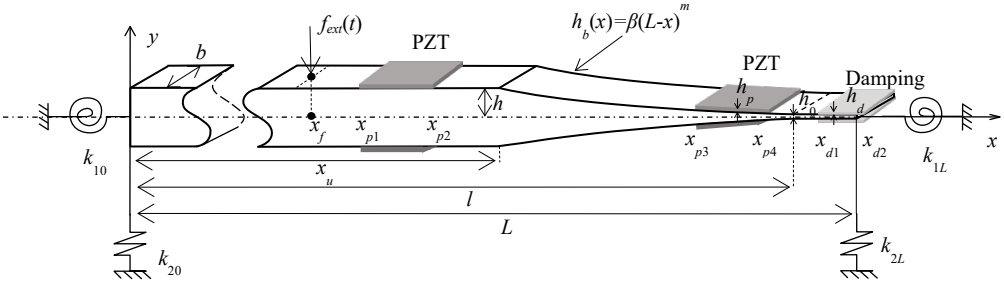

Figure 1: An ABH beam with symmetrical and power-law thickness profile, containing a uniform platform at the tip. Damping layers and PZT patches connected with external shunts are installed as coating on both side of the beam.

Consider the beam shown in Figure 1. The beam, with a constant width b and a total length L, is composed of a uniform portion with a constant thickness $2h_u$ and an ABH portion. The ABH portion contains a segment with a power-law profiled thickness ($2h_b$) from x_u to l, *i.e.*, $h_b(x)=\beta(L-x)^m$, and an extended platform of uniform thickness h_0 till L. The beam is symmetrical with respect to the mid-line of the beam. Single or multiple piezoelectric patches and damping layers, of constant thickness h_p and h_d, respectively, are symmetrically placed on both the top and bottom surfaces of the beam. The boundary conditions of the beam are simulated by a set of rotational and translational springs on each end of the beam. In particular, assigning sufficiently large values to k_{10} (rotational stiffness) and k_{20} (translational stiffness) at the uniform end of the ABH beam, and setting the two stiffness values k_{1L} and k_{2L} to 0 at the free end would mimic a cantilever beam [9]. The whole system under investigation undergoes flexural vibration under a point force excitation $f_{ext}(t)$ at x_f.

External electrical modules are designed and connected to the PZT patches to form a complete set of fully coupled electromechanical system. Single- or multi-DOF linear and nonlinear electrical shunts are designed to deliver different functionalities (either for ET or DA purposes), as shown in Figure 2.

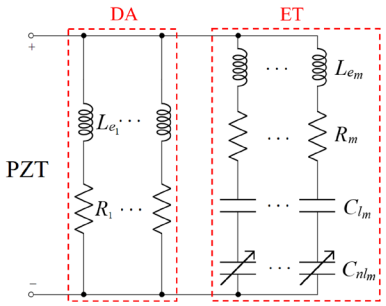

Figure 2: Schematic diagram of multiple piezoelectric transducers with multiple-DOF nonlinear electrical shunts.

In our previous work [8], a fully coupled electromechanical ABH model was developed via Rayleigh-Ritz approach with PZT patches connected a single-DOF nonlinear circuit. For the completeness of the study, the previous model is briefly recalled with the addition of multi-branched and multi-DOF circuits. The out-of-plane displacement $w(x, t)$ of the beam is still decomposed into a set of assumed admissible shape functions (modified trigonometric functions with supplementary boundary smoothing terms as detailed in [10]), the corresponding temporal coordinates (packed into an unknown vector $\mathbf{a(t)}$), the kinetic energy, potential energy and the work done by the external force $\mathbf{f}_{ext}\mathbf{(t)}$ and electric charge $\mathbf{q(t)}$ can all be mathematically expressed to form the Lagrangian. The coupled equations can be cast into the following matrix form:

$$\begin{bmatrix} \boldsymbol{M} & \\ & \boldsymbol{L_e} \end{bmatrix}\begin{bmatrix} \ddot{\boldsymbol{a}}(\boldsymbol{t}) \\ \ddot{\boldsymbol{q}}(\boldsymbol{t}) \end{bmatrix} + \begin{bmatrix} image(\boldsymbol{K})/\omega & \\ & \boldsymbol{R} \end{bmatrix}\begin{bmatrix} \dot{\boldsymbol{a}}(\boldsymbol{t}) \\ \dot{\boldsymbol{q}}(\boldsymbol{t}) \end{bmatrix} + \begin{bmatrix} real(\boldsymbol{K}) + \sum_{i=1}^{m} \vec{\boldsymbol{\Theta}}_i \vec{\boldsymbol{\Theta}}_i^{\,T}/C_{eq_i} & -\vec{\mathbf{Z}} \\ -\vec{\mathbf{Z}}^{\boldsymbol{T}} & \boldsymbol{Y} \end{bmatrix}\begin{bmatrix} \boldsymbol{a}(\boldsymbol{t}) \\ \boldsymbol{q}(\boldsymbol{t}) \end{bmatrix} + \begin{bmatrix} \mathbf{0} & \\ & \boldsymbol{C_{nl}}^{-1} \end{bmatrix}\begin{bmatrix} \vec{\mathbf{0}} \\ \boldsymbol{q}^3(\boldsymbol{t}) \end{bmatrix} = \begin{bmatrix} \boldsymbol{f}_{ext}(\boldsymbol{t}) \\ \mathbf{0} \end{bmatrix} \quad (1)$$

where

$$\mathbf{L_e} = \begin{bmatrix} L_{e_1} & & & \\ & L_{e_2} & & \\ & & \ddots & \\ & & & L_{e_m} \end{bmatrix},\ \mathbf{R} = \begin{bmatrix} R_1 & & & \\ & R_2 & & \\ & & \ddots & \\ & & & R_m \end{bmatrix},\ \mathbf{C_{nl}} = \begin{bmatrix} C_{nl_1} & & & \\ & C_{nl_2} & & \\ & & \ddots & \\ & & & C_{nl_m} \end{bmatrix},\ \mathbf{Y} = \begin{bmatrix} 1/C_{eq_1} & & & \\ & 1/C_{eq_2} & & \\ & & \ddots & \\ & & & 1/C_{eq_m} \end{bmatrix},$$

$$\vec{\mathbf{Z}} = \begin{bmatrix} \vec{\mathbf{\Theta}}_1/C_{eq_1} & \vec{\mathbf{\Theta}}_2/C_{eq_2} & \dots & \vec{\mathbf{\Theta}}_m/C_{eq_m} \end{bmatrix}.$$

in which $\mathbf{M}$ and $\mathbf{K}$ with subscripts stand for different components from the mechanical ABH beam which form the global mass matrix and stiffness matrix. $\mathbf{\Theta}$ is the electromechanical coupling matrix and C_{eq} the capacitance of the PZT equivalent circuit. $\mathbf{T}$ denotes the transpose of a matrix. Besides, L_e is the inductance, R is the resistance and C_{nl} is the nonlinear capacitance of the external circuit.

The frequency-domain solution of this model can be obtained by Harmonic Balance Continuation method [11], coupled with a continuation strategy, proven to be effective for solving multi-DOF nonlinear systems. Meanwhile, time-domain responses can be calculated by Newmark's method, which is widely used to solve nonlinear problems, details of which are described in [12].

3. Numerical Analyses

A cantilever ABH beam is numerically investigated. The mechanical part (ABH) has the same configuration as the one used in our previous paper [11] for easy comparisons. Material and geometrical parameters of the beam, PZT, damping and electrical shunts are listed in Table 1. The ABH beam is subjected to a harmonic point force excitation of 1N in amplitude at the point x_f=0.1m on the uniform portion. The beam displacement, quantified by $20\log_{10}$(Displacement) expressed in dB, is calculated at different observation positions on the beam (either on the uniform portion or the ABH portion) for structural response assessment.

Table 1. Material and geometrical parameters of the beam, damping, PZT and electrical shunt

Material parameters	**Geometrical parameters**
Beam Density: ρ_b=7800kg/m^3 Damping loss factor: η_b=0.005 Elasticity modulus: E_b=210GPa Damping Density: ρ_d=950kg/m^3 Damping loss factor: η_d=0 Elasticity modulus: E_d=5GPa PZT Density: ρ_p=7600kg/m^3 Damping loss factor: η_p=0 Elasticity modulus: E_p=132GPa Piezoelectric stress constant: e=-3C/m^3 Dielectric constant: ε^s=2.8×10^{-9}F/m Electrical shunt Inductance: L_e=1.895H Resistance: R=10Ω	Beam β=0.1 m=2 b=0.05m x_u=0.25m l=0.45m L=0.5m h_u=6.25mm h_0=0.5mm Damping x_{d1}=0.48m x_{d2}=0.5m h_d=0.5mm PZT x_{p1}=0.42m x_{p2}=0.48m h_p=0.5mm

3.1 Enhancing energy transfer

In this section, one set of PZTs connected to the nonlinear resonant shunt with a linear negative capacitance (Figure 3(a)) is firstly placed on the cantilever ABH beam to achieve enhanced ET effect through increasing the electromechanical coupling strength. In the present case, the cut-on frequency f_c [11] of the ABH beam is 940Hz, starting from which systematic ABH effects appear. Therefore, we choose the fourth mode before the cut-on frequency as the design and analysis target. PZT patches are placed at the position where the fourth modal deformation is the largest, *i.e.*, 0.42-0.48m, to generate the strongest electro-mechanical coupling between the PZT and the host beam. Targeting the fourth mode, the linear inductance L_e is set to 0.1H with a linear negative capacitance C_l=-3.57×10^{-8}C/V, the value of the resistance and the nonlinear capacitance are R=10Ω and C_{nl}=1×10^{-22}C^3/V, respectively.

The displacement spectrum of the ABH beam under different electrical conditions are considered to examine the outcome of the enhanced electromechanical coupling in term of ET effect, as shown in Figure 3(b). Frequency response curves are obtained upon imposing a sinusoidal excitation force with an amplitude of 1N sweeping form 0 to 1000Hz within 200 seconds. The corresponding frequency spectrum is obtained using the entire time-domain response signal through Fast Fourier Transform. Since the excitation frequency ends at 1000Hz, vibration signals which are higher than 1000Hz in the spectrum can be regarded as the energy transferred from the low frequencies before 1000Hz, used as the indicator of the energy transfer phenomenon. Here, the beam displacement is measured at x_m=0.45m on the ABH portion. In order to better show the ET process, the damping of the damping layers is deactivated (η=0).

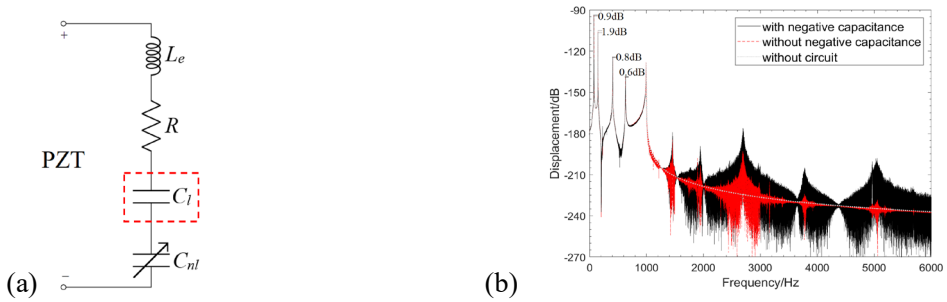

Figure 3: (a) Schematic diagram of nonlinear shunt with a linear negative capacitance; (b) Comparison of beam displacement spectra with different electrical circuits.

Figure 3(b) shows that high-frequency resonance peaks emerge after 1000Hz after the deployment of the electrical shunt, with or without the negative capacitance. Obviously, the high-frequency energy level of the system with the negative capacitance is further increased after 1000Hz: an increase of the peak levels alongside a spreading out of the energy distribution. Besides, the result also shows a further reduction in the amplitudes of the first four resonance peaks before f_c, amounting to 2dB reduction compared to the system without electrical shunt. This can also attribute to the fact that part of the low frequency energy is transferred to higher frequencies due to the enhanced nonlinear strength in the system.

3.2 Maintaining dynamic absorber

The numerical examples in the previous section demonstrate that, although the nonlinear shunt with the negative capacitance entails effective and beneficial ET to higher frequencies, the direct effects of the shunting on low frequency resonant vibration reductions are rather marginal. Therefore, in this section, we will explore ways to enhance the ET while maintaining the dynamic absorber (DA) effect to cope with the vibration mitigation at low-frequencies. Here, we still take a single set of piezoelectric shunts as an example to illustrate the idea. To tackle the problem, a linear electrical resonant branch is added to the previous nonlinear shunt, as shown in Figure 4(a). The linear branch is designed to target one structural resonance through creating classical DA effects, while the remaining nonlinear branch is used for ET. Here, in order to more clearly compare the precise impact of the DA effect on high-frequency energy, the vibration responses are indicated by the envelopes of the beam displacement spectra.

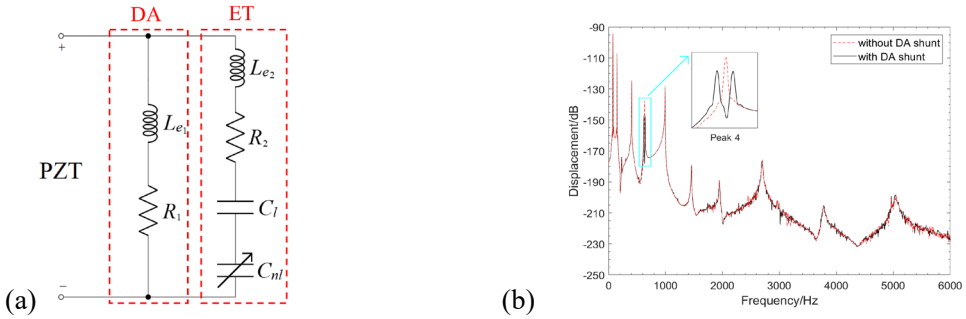

Figure 4: (a) Schematic diagram of nonlinear shunt with two electrical branches containing different functions; (b) Comparison of beam displacement spectrum envelopes with and without DA shunt.

Figure 4(b) shows the displacement spectrum envelopes of the beam used above with and without the additional DA branch in the electrical shunt. The linear DA branch is designed to target the fourth mode of the beam. It can be seen that the addition of the linear DA branch exerts nearly no effect on the high-frequency vibration caused by the previously observed ET. However, typical DA effects are apparent, which leads to a split of the resonance peak and a significant reduction (close to 10dB) of the vibration level, as shown by the enlarged view of the fourth peak. This way, even in the presence of a strong electrical nonlinearity, dynamic absorber effect can still be maintained in the system owing to the linear DA branch of the shunt. Interesting enough, the two bunches, linear and nonlinear, do not seem to interfere much with each other, reflecting a weak coupling between them. The benefit of this observation is that each branch can be designed separately and tactically to achieve their respective functions: linear part for low-frequency DA effect and the nonlinear part for cross-frequency ET effect. This solution allows for alleviating the detuning problem of the nonlinear shunts for low-frequency vibration mitigation, and the avoidance of linear DA failure in the presence of strong nonlinearity in the electrical shunts.

3.3 Comprehensive design

The above analyses demonstrate the possibility of enhancing the cross-frequency energy transfer by increasing the electromechanical coupling strength through different methods while maintaining the dynamic absorber effect to cope with low-frequency vibrations through adding the additional electrical branch. In this section, we will deploy this combined ET and DA design methodology and apply different strategies to different frequency bands to finally achieve broadband multimodal vibration mitigation.

The underlying rationale which guides the electrical shunt design is schematically illustrated in Figure 5(a) to cope with specific mitigation philosophies adopted for different frequency ranges. When a damping module is deployed over the ABH portion including the extended platform region, systematic ABH effects are expected above the cut-on frequency of the ABH, denoted by f_c, thus generating high damping and energy dissipation. Therefore, the high-frequency energy after f_c (inherent in this region or transferred from low frequencies to be demonstrated later) can be naturally dissipated by the ABH-enhanced damping effects. Before f_c, ABH effect is marginal, the vibration benefit would mainly rely on the electrical shunt. From $1/3f_c$ to f_c, the shunt design will capitalize on both the ET effects of nonlinear shunts and the DA effects from the linear branch. ET branches are deployed to transfer the energy of the dominant harmonics (starting from the third harmonic onwards) to a higher frequency region to trigger the same energy dissipation process as the previous case (exceed the frequency barrier imposed by f_c), and DA branches are used to simultaneously reduce their own resonant responses. For the ultra-low frequency range, those modes with natural frequencies $f_n<1/3f_c$, vibration mitigation would mainly rely on the DA effects. This is because even with ET, the transferred energy to the third harmonic would still be lower than f_c, which is still not enough to trigger meaningful ABH effects.

As an example, following the above design philosophy, the electrical shunts are designed to target the first four modes (before f_c) of the ABH beam in Section 3.1 and 3.2. For the 3rd and 4th modes in the frequency range from $1/3f_c$ to f_c, electrical branches will be designed to generate ET in the surrounding frequencies to a higher frequency region (above f_c), meanwhile, DA effects are also embedded for these two modes. As to the first two modes (natural frequencies $f_n<1/3f_c$), the vibration mitigation has to totally rely on the DA effects. The circuit diagrams in the piezoelectric shunts are shown in Figure 5(b), and the corresponding circuit parameters are shown in Table 2.

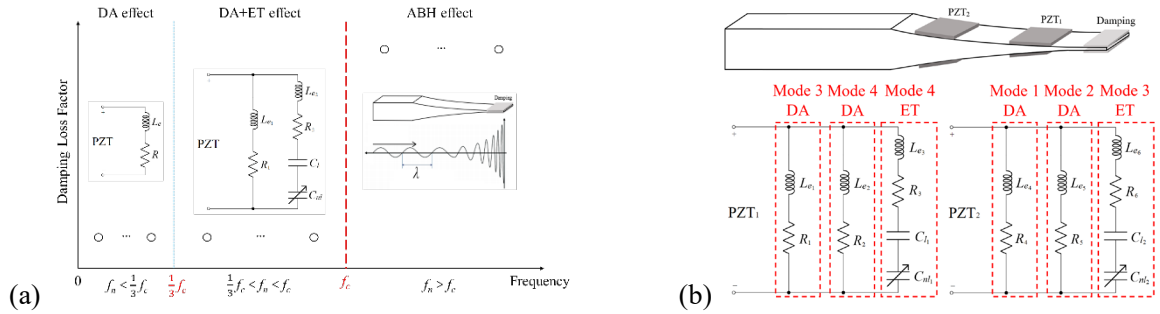

Figure 5: (a) Design philosophy for achieving broadband multimodal vibration mitigation in the electromechanical ABH beam; (b) Schematic diagram of comprehensive design.

Table 2. Electrical parameters of designed circuit

Electrical parameters
Inductance L_{e1}=4.728H L_{e2}=1.688H L_{e3}=0.02H L_{e4}=81.4H L_{e5}=13.65H L_{e6}=0.02H
Resistance R_1=150Ω R_2=20Ω R_3=10Ω R_4=400Ω R_5=100Ω R_6=10Ω
Capacitance C_{l1}=-3.4005×10^{-8}F C_{l2}=-5.6399×10^{-8}F C_{nl1}=1×10^{-22}C^{3}V^{-1} C_{nl2}=1×10^{-22}C^{3}V^{-1}

Analyses on the achieved results are conducted in two stages. Firstly, in order to better show the ET process, the damping of the damping layers is deactivated (η=0). Displacement spectra of the beam with and without the circuit are shown and compared in Figure 6(a), which displays the expected ET effect to high frequencies and the DA effect for low-frequency modes. More specifically, compared with the system without shunts, vibration increases significantly in the targeted ET region beyond 1000 Hz, as evidenced by the significant increase in the energy level (due to the absence of the damping in the damping layers). Meanwhile, significant DA effects take place and split the first four resonant peaks apart, typical of DA effects, to yield a significant vibration reduction, ranging roughly from 16dB to 50dB.

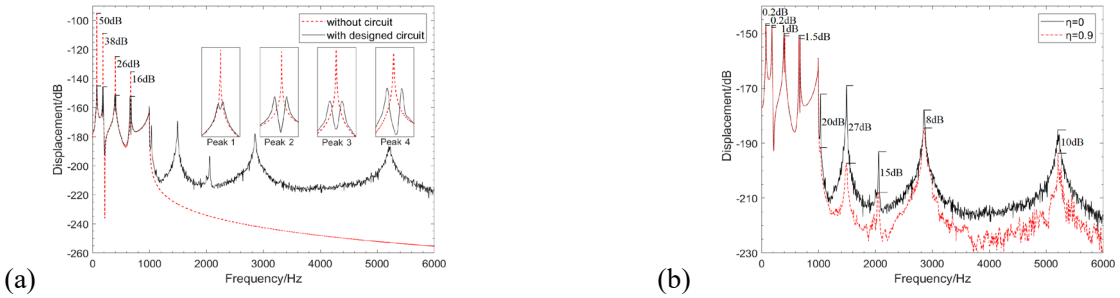

Figure 6: Comparison of beam displacement spectrum envelopes (a) without circuit and with designed circuit; (b) with different damping ratio η.

The damping of the damping layers is then activated through setting η=0.9. This helps better apprehend the complete ABH process. Comparisons between the two cases (η=0, 0.9) are made in Figure 6(b). It can be seen that the activated damping effectively absorbs the transferred energy in the high frequency region above fc, leading to a significant vibration reduction there. The reduction is particularly impressive in the range of 1000-2000Hz amounting to 27dB, where locate the third harmonics of the 3rd and the 4th modes. Note the addition of the damping does not obviously jeopardize the vibration reduction of the lower-order resonances, although a slight reduction up to 1.5 dB is noticed. The observed vibration reduction due to the addition of the damping layer reflects the entire ABH process, which is enhanced by the electrical nonlinearity through effective ET. The outcome of the overall electromechanical ABH process, owing to the combined DA and ET effects lower the effective frequency range of the ABH, allowing for broadband vibration mitigation.

4. Conclusions

The content of this paper falls into our general efforts in imposing intentional electrical nonlinearities via PZT patches over an ABH beam to tactically influence its dynamics through electromechanical coupling for achieving broadband vibration mitigation. To overcome the limitations of the existing single-branched nonlinear shunt, we firstly propose to enhance the cross-frequency energy transfer (ET) in the ABH beam through increasing the electromechanical coupling strength by using introducing a negative capacitance in the nonlinear shunt. Numerical examples show enhanced ET, despite rather marginal reduction of low frequency resonant vibration. To tackle the problem, linear electrical resonant branches are added to the nonlinear shunt to generate dynamic absorber (DA) effects without compromising the nonlinearity-dominated ET. It is demonstrated that the two parallelly arranged branches in a shunt, linear and nonlinear, are weakly coupled and can be separately designed to target particular modes to achieve pre-set functionalities. More specifically, we provide a comprehensive design example, which embraces the principle of ET and DA, deployed to cope with different frequency bands.

More specifically, the proposed vibration mitigation method roots in the following rationale. 1). High-frequency vibration energy, typically above f_c, can be naturally dissipated by the ABH-enhanced damping in the system, exemplified by a small amount of damping materials placed at the ABH tip region. 2). For the frequency range below but relatively close to f_c, typically from $1/3f_c$ to f_c, nonlinear electrical shunts can be deployed to achieve ET to a higher frequency region (above f_c) so that the same energy dissipation process (summarized in 1) above) can be subsequently triggered. 3). For the lower-order resonant modes, vibration mitigation would mainly rely on the DA effects achieved through the linear resonant branches in the shunt. Note DA effects can also be imposed to these modes belonging to the category 2) above without sensibly affecting the expected ET. The outcome of this comprehensive design is the breaking down of the frequency barrier existing in conventional linear ABH structures, and appreciable broadband multi-modal vibration mitigation at low frequencies.

Acknowledgements

Authors thank the Research Grant Council of the Hong Kong SAR (PolyU 152023/20E) for financial support.

REFERENCES

[1] A. Pelat, F. Gautier, S.C. Conlon, F. Semperlotti, The acoustic black hole: A review of theory and applications, *J. Sound Vib.*, 476 (2020) 115316.

[2] M. Mironov, Propagation of a flexural wave in a plate whose thickness decreases smoothly to zero in a finite interval, *Sov. Phys. Acoust.*, 34 (1988) 318-319.

[3] V.V. Krylov, New type of vibration dampers utilising the effect of acoustic black holes, *Acta Acust. united Ac.*, 90 (2004) 830-837.

[4] H. Ji, W. Huang, J. Qiu, L. Cheng, Mechanics problems in application of acoustic black hole structures, *Adv. Mech.*, 47 (2017) 333.

[5] L. Tang, L. Cheng, Enhanced acoustic black hole effect in beams with a modified thickness profile and extended platform, *J. Sound Vib.*, 391 (2017) 116-126.

[6] J.Y. Lee, W. Jeon, Vibration damping using a spiral acoustic black hole, *J. Acoust. Soc. Am.*, 141 (2017) 1437-1445.

[7] H. Li, C. Touzé, F. Gautier, A. Pelat, Linear and nonlinear dynamics of a plate with acoustic black hole, geometric and contact nonlinearity for vibration mitigation, *J. Sound Vib.*, 508 (2021) 116206.

[8] L. Zhang, G. Kerschen, L. Cheng, Nonlinear features and energy transfer in an Acoustic Black Hole beam through intentional electromechanical coupling, *Mech. Syst. Sig. Process.*, 177 (2022) 109244.

[9] L. Tang, L. Cheng, H. Ji, J. Qiu, Characterization of acoustic black hole effect using a one-dimensional fully-coupled and wavelet-decomposed semi-analytical model, *J. Sound Vib.*, 374 (2016) 172-184.

[10] L. Zhang, G. Kerschen, L. Cheng, Electromechanical coupling and energy conversion in a PZT-coated acoustic black hole beam, *Int. J. Appl. Mech.*, 12 (2020) 2050095.

[11] T. Detroux, L. Renson, L. Masset, G. Kerschen, The harmonic balance method for bifurcation analysis of large-scale nonlinear mechanical systems, *Comput. Method. Appl. M.*, 296 (2015) 18-38.

[12] S.Y. Chang, Studies of Newmark method for solving nonlinear systems: (I) basic analysis, *J. Chin. Inst. Eng.*, 27 (2004) 651-662.